HOSTED BY

ELSEVIER

Available online at www.sciencedirect.com

ScienceDirect

Resource-Efficient Technologies 2 (2016) 133–142

www.elsevier.com/locate/reffit

Research paper

On the behaviour, mechanistic modelling and interaction of biochar and crop fertilizers in aqueous solutions

Prithvi Simha [a,b], Ashish Yadav [c], Dipak Pinjari [c], Aniruddha B. Pandit [c,*]

[a] Department of Environmental Sciences and Policy, Central European University, Nádor utca 9, 1051 Budapest, Hungary

[b] School of Earth, Atmospheric and Environmental Sciences (SEAES), The University of Manchester, M13 9PL Manchester, United Kingdom

[c] Department of Chemical Engineering, Institute of Chemical Technology, Matunga, Mumbai 400 019, India

Received 23 April 2016; received in revised form 28 July 2016; accepted 30 July 2016

Available online 25 August 2016

Abstract

Although the benefits of applying biochar for the purposes of soil conditioning and crop productivity enhancement have been demonstrated, relatively few studies have elaborated on its causal mechanisms, especially on the biochar–fertilizer interaction. Thus, in the present study, the ex-situ adsorptive potential of base activated biochar (BAB) towards plant nutrient immobilization and removal from aqueous solutions was investigated. Napier grass (*Pennisetum purpureum*) was utilized as the precursor to prepare slow vacuum pyrolysed char and its affinity towards adsorption of urea was examined at various process conditions. Low sorption temperatures, moderate agitation speeds and high initial concentration were seen to favour greater urea uptake by BAB. The sorption was exothermic, physical, spontaneous and had a pseudo-second order kinetic fit. Both surface and intra-particle diffusion governed the removal and immobilization of urea. Furthermore, process mass transfer was limited by film diffusion of urea to the external surface of the BAB. Equilibrium studies suggested that Dubinin–Radushkevich is the most appropriate model to describe the urea-BAB behaviour with maximum uptake, estimated to be 1115 $mg \cdot g^{-1}$. Through such ex-situ analysis, it could be possible to have prior knowledge, quantification and differentiation of the potential of chars manufactured from various feedstocks. This could then be used as an effective screening step in designing appropriate biochar–fertilizer systems for soil conditioning and help reduce the time and effort spent otherwise in long-term field studies.

Keywords: Soil fertility; Adsorption; Soil management; Sustainable agriculture; Fertilizer; Adsorption kinetics

1. Introduction

Biochar is a highly carbonaceous charred organic material that is deliberately applied as a soil conditioner with the intent to improve soil quality and associated environmental services [1]. Its preparation requires pyrolysis of plant-derived biomass under limited or no oxygen to promote the thermal degradation of the precursor. Several studies have pointed out that the application of biochar for soil conditioning, fertilization and amendment is a 'multiple-win' strategy [2] with the most touted benefits being carbon sequestration, waste disposal, enhanced plant nutrient uptake, pollutant immobilization and simultaneous biofuel production [3]. Nonetheless, biomass pyrolysis is not a new technology as it has conventionally been applied to maximize bio-liquid production for renewable energy capture. Moreover, with the char derived from the process potentially attaining energy contents as high as 30 $MJ \cdot kg^{-1}$ [4], any process that favours the char over the fuel represents an opportunity cost [5].

On the contrary, it is also evident today that immediate and effective adaptation measures need to be implemented for human society to address as well as mitigate the consequences of anthropogenic-induced radiative forcing and climate change. The causal linkage between agriculture and climate change has been shown to result in a net radiative forcing of 13.5% with crop production related land-use change accounting for a further 17.4% [6]. Additionally, the continuous intensification of agricultural practices in the hope of attaining global food security has caused extensive deterioration of soil quality and fertility [7]. It is therefore imperative that workable and implementable technologies are adopted that simultaneously

* Corresponding author. Department of Chemical Engineering, Institute of Chemical Technology, Matunga, Mumbai 400 019, India. Fax: +91-22-33611020.

E-mail address: ab.pandit@ictmumbai.edu.in (A.B. Pandit.).

http://dx.doi.org/10.1016/j.reffit.2016.07.006

Nomenclature

C_e	liquid-phase concentration of urea at equilibrium ($mg \cdot L^{-1}$)
C_t	liquid-phase concentration of urea at any time t ($mg \cdot L^{-1}$)
C_0	liquid-phase concentration of urea at t = 0 ($mg \cdot L^{-1}$)
D_i	effective diffusion coefficient ($m^2 \cdot min^{-1}$)
F	fractional attainment of equilibrium expressed as a ratio of q_t to q_{max}
K_a	Flory–Huggins isotherm constant ($L \cdot g^{-1}$)
k_{ad}	Dubinin–Radushkevich isotherm constant ($mol^2 \cdot kJ^{-1}$)
k_{id}	intra-particle diffusion rate constant ($mg \cdot g^{-1} \cdot min^{-1/2}$)
k_1	first order rate constant (min^{-1})
k_2	second order rate constant ($g \cdot mg^{-1} \cdot min^{-1}$)
K_F	Freundlich isotherm constant ($mg \cdot g^{-1} \cdot (L \cdot mg^{-1})^{1/n}$)
K_L	Langmuir isotherm constant ($L \cdot mg^{-1}$)
S_s	BAB surface area per unit volume of particle-free adsorbate (cm^{-1})
m	BAB loading per unit volume of particle-free adsorbate
n	number of experimental observations
q_e	urea uptake capacity of BAB at equilibrium ($mg \cdot g^{-1}$)
$q_{e(exp)}$, $q_{e(pred)}$	experimental and predicted urea uptake capacity of BAB at equilibrium ($mg \cdot g^{-1}$)
q_m	maximum monolayer urea sorption ($mg \cdot g^{-1}$)
q_s	Dubinin–Radushkevich theoretical maximum sorption capacity ($mg \cdot g^{-1}$)
q, q_t	amount of urea adsorbed by BAB at any time t ($mg \cdot g^{-1}$)
R_L	separation factor, Langmuir model
Ss	outer adsorbent surface per unit volume of particle-free sorbate (cm^{-1})
t	sorption time (min)
T	absolute temperature (K)
V	volume of adsorbate solution (L)
W	mass of BAB used (g)
β_L	mass transfer coefficient ($cm \cdot sec^{-1}$)
ε	Polanyi potential
θ	degree of surface coverage

provide pathways for improving (or restoring) soil health and mitigating climate change. Lehmann [8] estimated that carbon abatement to the (realistic) extent of 1 $GtC \cdot year^{-1}$ can be achieved through the addition and concentration of carbon within soils as biochar; this stems from our understanding that biochar could act as permanent C sinks (half-life of 100–1000 years) due to their chemical persistence within soils [8]. In addition, the co-benefits of biochar soil amendment include improved nutrient retention, augmented soil-moisture holding capacity, reduced emissions of CH_4 and N_2O, higher cation exchange capacity, etc. [9,10].

In particular, several investigations into the agronomic value of biochar addition have indicated an increase in crop yield following soil conditioning [11–14]. However, this increase in crop productivity was the combined interactive effect of biochar and externally added N fertilizers. For instance, Chan et al. [12] observed that there was no significant effect of biochar addition on productivity in the absence of N fertilizers. The same authors also demonstrated a corresponding increase in productivity as biochar addition was increased in the presence of N fertilizers. Similar observations on the inherent dependency of biochar on external fertilizer additions for augmenting crop growth have been made by Van Zwieten et al. [15] in their studies on wheat and radish biomass yields. However, little research exists on the causal mechanisms that govern and determine the much acclaimed benefits of biochar and its ability to immobilize plant available N. Particularly, few studies have evaluated the ex-situ adsorptive potential of biochar towards nutrient adsorption. While the benefits of biochar addition to soils are well-recognized today, there is a dearth of literature that seeks to qualitatively and quantitatively distinguish various feedstock derived biochar. Ex-situ understanding and quantification of the potential of different chars to adsorb soil nutrients could act as a screening process for identifying a good combination of biochar and crop fertilizer for improving soil health. Therefore the objective of the present work is to investigate the adsorptive characteristics of biochar to elucidate its relative affinity towards nitrogenous fertilizers. Through the analysis of urea (fertilizer) sorption from aqueous solutions onto a plant biomass derived char, the processes behaviour, rate controlling mechanisms, mass transfer and establishment of equilibrium have been described. Such quantification could potentially allow for designation of the agronomic values of biochar derived from various feedstocks and lead to their large scale application.

2. Materials and methods

2.1. Biochar preparation and characterization

Napier grass (*Pennisetum purpureum*) was utilized as the precursor for biochar production and was obtained from Kirloskar Oil Engines Ltd., Pune, India. Initially, the grass was uniformly ground to a particle size of 1–1.5 mm in an electric mixer and oven dried at 105 °C until constant weight was obtained. Subsequently, 50 g of the oven dried grass was fed to a SS 316 batch reactor and vacuum pyrolysed at 400 °C (based on initial experiments). A pressure gauge (1–15 bar) and a thermostat (K-type sensor) were attached to the reactor to monitor the pyrolysis. The obtained biochar was further washed with KOH (1:2) and activated at 500 °C as per the procedure described by Tseng and Tseng [16] in order to enhance its sorption capacity. Finally, it was acid washed (0.1 M HCl) to a pH of ca. 6–7 and dried in oven at 105 °C. The obtained biochar (BAB) was stored in air-tight polypropylene containers for further use and analysis.

Prior to activation, the char was characterized for its pH, electrical conductivity (Jenway-4510, Staffordshire, UK) and ash composition (heating in muffle furnace at 800 °C) as described elsewhere [17,18]. Water retention capacity of the char was calculated by adding it in various loading rates (1–5%, w/w) to a suspension of soil (20 g) and water (20 mL) that was stirred for 24 h. Subsequently, the suspension was filtered and the residual weight was used as the measure of the water retention. The elemental composition of the biochar was estimated using an elemental analyser (Perkin-Elmer 240B, USA). Furthermore, following the activation of the char, its surface functional groups were determined by Fourier transform infrared spectroscopy (FTIR-2000, PerkinElmer, USA) using spectrograde KBr at 4 cm^{-1} of resolution and 64 scans·min^{-1} between 4000 and 400 cm^{-1}. Field emission gun scanning electron microscopy (FEG-SEM) was performed by coating BAB with platinum and recording its microstructures at 15 mA and accelerating voltage of 10 kV (JEOL JSM-7600F, Japan).

2.2. Adsorption experiments

Urea stock solutions were prepared in 250 mL Erlenmeyer flasks with various concentrations: 0.3, 0.45, 0.6, 0.9, 1.2, 1.5 and 2 g·L^{-1}. Adsorption was performed in electric thermostated shaker with a fixed BAB loading of 0.125 g at various shaker speeds (100, 125, 150, 175 and 200 rpm) and temperatures (25, 35 and 45 °C). At different time intervals, 1 mL aliquots were withdrawn from the shaker, filtered through a 0.45 µm syringe and analysed for change in urea concentration by determining the corresponding change in absorbance at 430 nm [19] using a UV–visible spectrophotometer (Thermo-Fisher Scientific, USA). The urea uptake capacity (q_e; mg·g^{-1}) of the BAB was determined by Eq. (1), where C_0 and C_t (mg·L^{-1}) are urea concentration initially and at any time 't' (min), respectively; V (mL) is the volume of solution and W (g) is the amount of BAB added. The experiments were performed in duplicate and deviations were within 5%; statistical analysis was done with MATLAB® and average values have been used in all graphical representations. All chemicals and reagents were of analytical grade and used without any further purification.

$$q_e = \frac{(C_0 - C_t)V}{W} \tag{1}$$

2.3. Equilibrium isotherm, kinetics and mass transfer

In order to describe the dynamic separation of urea from the solution and onto the BAB, the establishment of sorption equilibrium was modelled through Langmuir, Freundlich, Flory–Huggins, and Dubinin–Radushkevich isotherms [20]. The experimental data were regressed against the linearized equations of the models. In order to determine the isotherm parameters and the best fit of experimental data against the model predictions, the coefficient of determination (R^2) was calculated and error analysis was carried out by estimating the normalized deviation (ND) and normalized standard deviations (NSD) as seen in Eqs. (2) and (3). $q_{e(exp)}$ and $q_{e(pred)}$ are the experimental and predicted urea sorption capacity (mg·g^{-1}), respectively, and n is the number of observations made.

$$ND = \frac{100}{n}\sum\left|\frac{q_{e(exp)} - q_{e(pred)}}{q_{e(exp)}}\right| \tag{2}$$

$$NSD = 100\sqrt{\frac{\sum\left(q_{e(exp)} - q_{e(pred)}\right)/q_{e(exp)}\right)^2}{n}} \tag{3}$$

Furthermore, the kinetics of urea uptake by the BAB was expressed using the first-order, second-order and intra-particle diffusion models as described elsewhere [21]. The rate of mass transfer of urea was determined by Eq. (4) as per the procedure detailed by McKay et al. [22]. K, a dimensionless parameter, was estimated as a product of the Langmuir isotherm constant (K_L; L·mg^{-1}) and its monolayer saturation capacity (q_m; mg·g^{-1}); S_s (cm^{-1}) is the BAB surface area per unit volume of particle-free adsorbate; m (g·L^{-1}) is the BAB loading per unit volume of particle-free adsorbate; and β_L (cm·min^{-1}) is the mass transfer coefficient determined through the slope of the plots of $\ln((C_t/C_0) - 1/(1 + mK))$ against time.

$$ln\frac{C_t}{C_0} - \frac{1}{1+mK} = ln\frac{mK}{1+mK} - \frac{1+mK}{mK}\cdot\beta_L S_s t \tag{4}$$

3. Results

3.1. Characterization

The yield of the pyrolysed biochar at 400 °C was found to be 45% and ash content evaluated at 800 °C was 5.2%. The biochar had a pH of 9.81 and electrical conductivity was 0.158 dS·m^{-1}. The elemental composition of the char obtained from Napier grass pyrolysis showed that it was free from sulphur; the constituents were C (54.6%), H (3.6%), N (2.9%) and O (6.7%). This resulted in a C:N ratio of 11.93 (i.e. <20), which is an indication of the char's ability to retain soil nutrients over time and hence improve soil fertility and crop productivity [23]. The O:C ratio was 0.17, which points to a minimum half-life of ~1000 years. Furthermore, the water retention capacity was found to increase from 13.6 to 30.5% as the amount of biochar applied increased from 1 to 5% (w/w); hence, addition of biochar to agricultural soils can increase water retention through reduced surface run-off and limit the loss of soil nutrients therein. Similar observations have been made by Beck et al. [24] as well as Laird et al. [25].

Fig. 1 illustrates the recorded FTIR spectra for Napier grass biochar. Before adsorption (Fig. 1(a)), distinct peaks were seen at 2925.11, 2370.01, 1600.01 and 803.22 cm^{-1} that correspond respectively to C—H off C═O, O—H stretch, N—H bend, C—O and C—H out of plane surface functionalities. Following urea adsorption onto the BAB, new spectra were seen at 3350.12, 1600 and 750.55 cm^{-1} which correspond to secondary amide N—H stretch; this is indicative of the potential presence of N on the char (Fig. 1(b)). The FEG-SEM images have been provided in Fig. 2. In comparison to the precursor (dried Napier grass) (Fig. 2(a)), the pyrolysed biochar (Fig. 2(b)–(d)) displayed irregular internal surface and good porosity. Pore sizes were found to span in the range of 10–50 µm and were indicative of the development of large internal surface for adsorption.

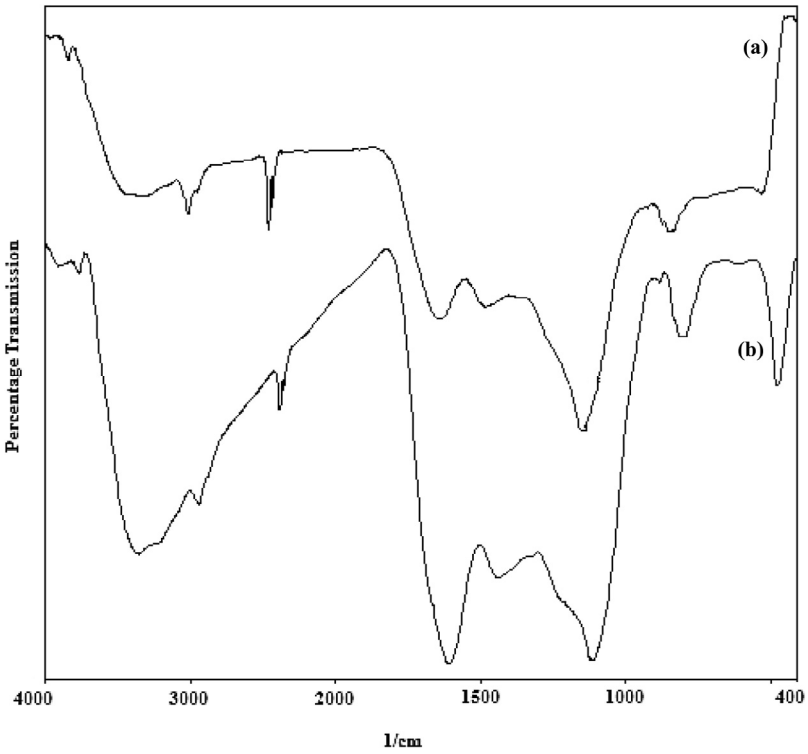

Fig. 1. FTIR spectra for (a) BAB before adsorption and (b) BAB after adsorption.

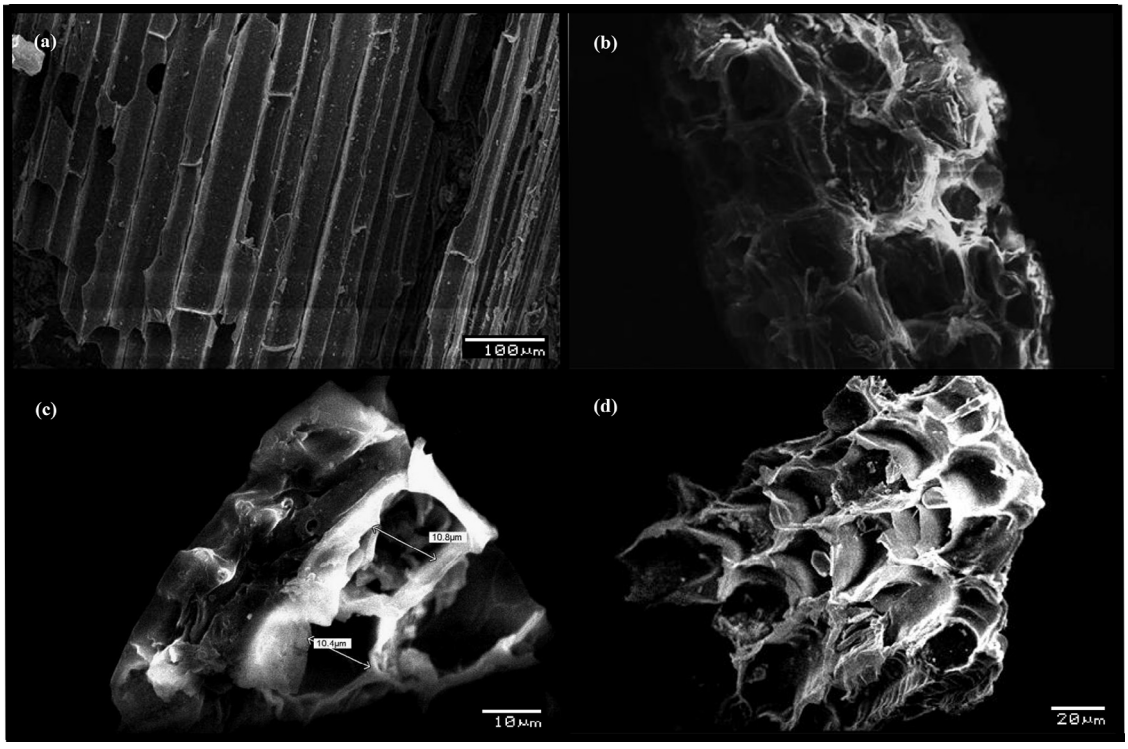

Fig. 2. FEG-SEM microstructures of Napier grass (a) and BAB (b–d).

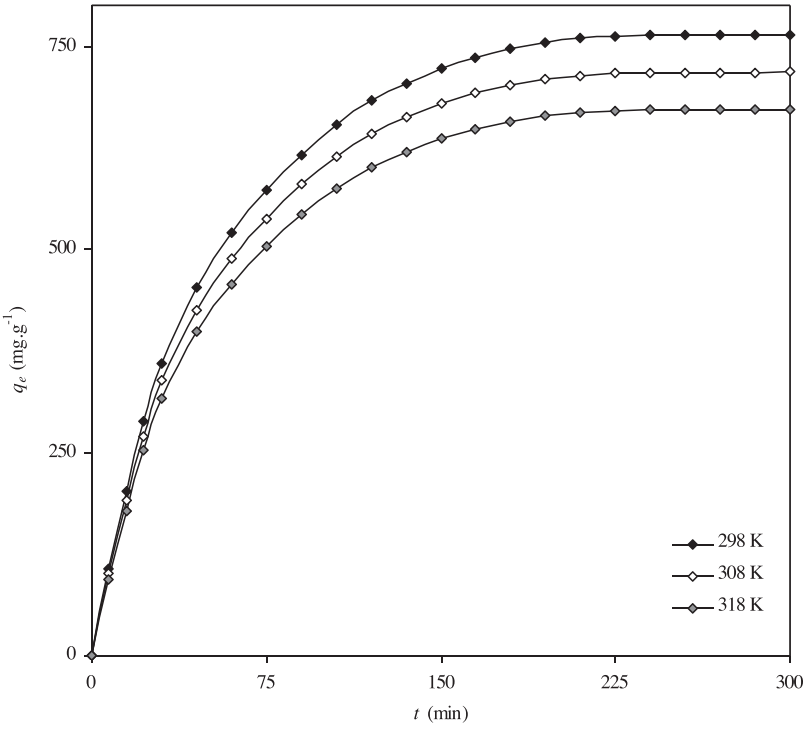

Fig. 3. Effect of temperature on urea sorption with initial concentration of 0.6 g·L^{-1} and shaker speed of 150 rpm.

3.2. Effect of temperature, agitation and concentration

Initially, the adsorptive characteristics of the BAB were tested at a fixed shaker speed of 150 rpm, initial urea concentration of 0.6 g·L^{-1} and at three different temperatures – 25, 35 and 45 °C – with the results illustrated in Fig. 3. As seen through the sorption capacity at equilibrium, lower temperatures favoured the sorption; q_e decreased by 12% from 760 to 672 mg·g^{-1} as temperature was raised from 25 to 45 °C. This indicated that the process was exothermic in nature and follows the corollary that, increasing the kinetic energy of sorbate molecules (urea) in the solution increases system entropy which, in turn, reduces the ability of urea to aggregate and adsorb over the BAB. Dąbrowski et al. [26] in their studies over phenolic adsorption as well as Chiang et al. [27] working with volatile organics have recorded similar observations. Hence, in all further experimental runs, the temperature was fixed at 25 °C.

As seen through Fig. 4, the speed of agitation in the shaker affected the mass transfer and removal of urea from the solution. Certainly, it does govern the distribution of urea within the solution and the formation of the external boundary film over the BAB surface. At 100 rpm, the equilibrium urea uptake by BAB was 760 mg·g^{-1} and increased to 912 mg·g^{-1} as the shaker speed was increased to 175 rpm. Furthermore, the increase in uptake was minimal (<1%) as speed was increased from 150 to 175 rpm. Any further increase resulted in decreased urea sorption. This is possibly due to the influence of desorption at higher speeds making the sorption reversible; increasing the speed beyond 175 rpm resulted in the spontaneous desorption of adsorbed urea from the BAB and hence reduced its net urea uptake capacity. The optimum shaker speed from these experimental runs was found to be 150 rpm.

The initial concentration of urea within the adsorbate solution strongly influenced the BAB uptake capacity as seen in Fig. 5. At 25 °C, increasing the concentration (0.3–2.0 g·L^{-1}) resulted in corresponding increase in uptake (from 385 to 1032 mg·g^{-1}). The time for establishment of equilibrium was 300 min. Furthermore, the curves were smooth at all concentrations studied pointing towards the possibility of monolayer adsorption on the BAB. The urea removal was rapid at the beginning ($t < 100$ min) as the process was driven forward by the large concentration difference between the sorbate and the sorbent; based on the smoothness of the curve, it could be assumed that urea forms a one-molecule thick layer over the BAB until 100 min. Gradually, this reduced with time as the sorption sites became saturated and any further uptake was possibly a result of pore diffusion from the external to the internal parts of the BAB. Similar observations have been made in other sorption systems [28,29].

3.3. Sorption kinetics and mass transfer

The interactions of all the process parameters with the sorption time were evaluated through dynamic kinetic studies and have been summarized in Tables 1–3. Better compliance ($R_2^2 > 0.97$) of the experimental and predicted urea uptake was seen for the second-order model to describe the effect of temperature (Table 1). Furthermore, given the exothermic nature of the process, the initial sorption rate (h) decreased with temperature and the minimum equilibrium sorption (q_2) was 763.35 mg·g^{-1} at 45°C. As Ho and McKay [30] observed, elevation of temperature may have increased the tendency of urea molecules to escape from the BAB interface and this suggests that the sorption may be physical in nature. Also, a linear relationship between k_2 and

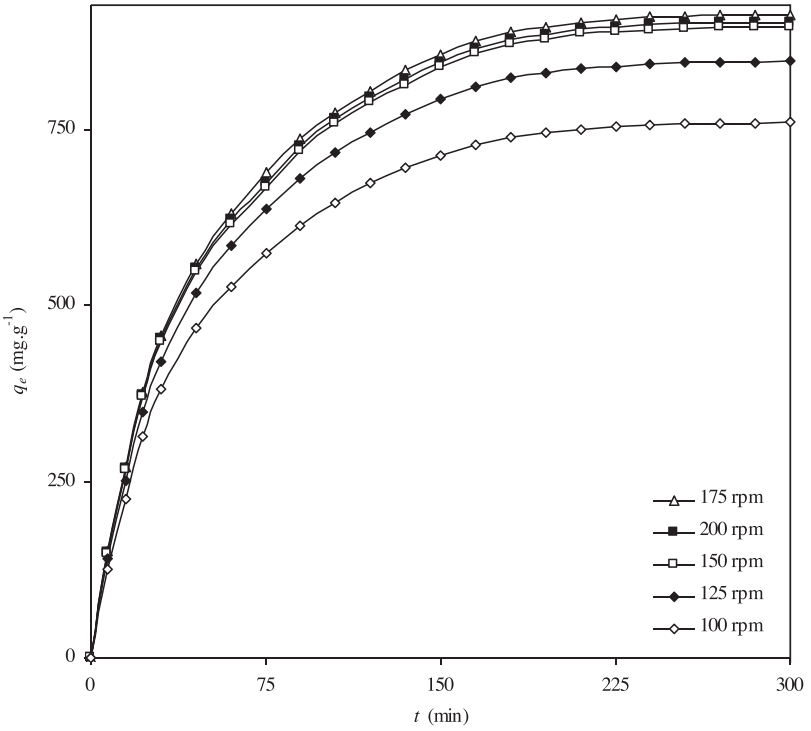

Fig. 4. Effect of speed of agitation on urea sorption at 25 °C and urea concentration of 0.9 g·L^{-1}.

temperature was seen by developing Arrhenius plots (not shown) and found to exhibit the following form (Eq. 5).

$$k_2 = 9.78\times10^{-4}\cdot exp\left(\frac{8.76E-03}{8.314\,T}\right) \quad (5)$$

The series of experiments to depict the effect of the speed of agitation (Table 2) indicated that the rate constant (k_2) increased from 2.11E–05 to 2.77E–05 with speed until 175 rpm. Furthermore, the increase in initial sorption rate was also found to be high for lower agitation speeds. An excellent agreement

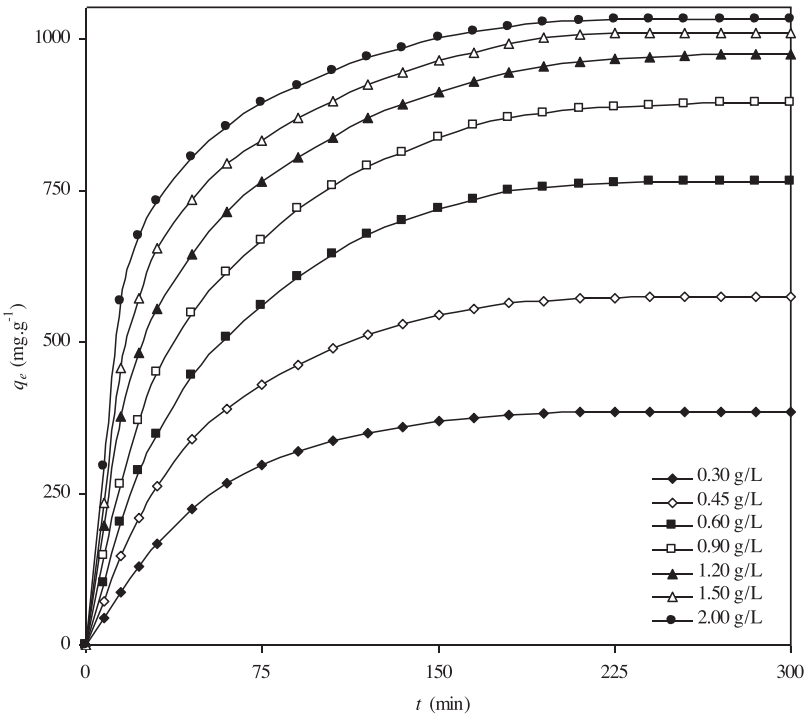

Fig. 5. Effect of concentration on urea uptake capacity of the BAB.

Table 1
Kinetic parameters for effect of temperature on urea sorption.

T	R_1^2	k_1	q_1	R_2^2	k_2	q_2	h	R_i^2	k_{id}
298	0.9611	0.0237	980.392	0.9761	2.85E−05	909.112	16.65	0.9032	45.23
308	0.9689	0.0232	894.541	0.9785	3.19E−05	833.333	16.49	0.9114	42.56
318	0.9621	0.0231	862.779	0.9831	3.56E−05	763.358	16.11	0.9085	39.76

Table 2
Kinetic parameters for effect of speed of agitation on urea sorption.

S	R_1^2	k_1	q_1	R_2^2	k_2	q_2	h	R_i^2	k_{id}
100	0.9839	0.02142	860.597	0.9985	2.11E−05	769.091	22.48	0.9034	43.40
125	0.9827	0.02144	967.386	0.9986	2.48E−05	844.000	24.80	0.9056	48.42
150	0.9779	0.02188	1053.416	0.9986	2.72E−05	901.510	26.18	0.9066	51.22
175	0.9787	0.02188	1065.614	0.9986	2.77E−05	911.111	26.79	0.9066	51.63
200	0.9779	0.02188	1061.940	0.9987	2.73E−05	895.596	26.26	0.9048	52.21

Table 3
Kinetic parameters for effect of initial concentration on urea sorption.

C	R_1^2	k_1	q_1	R_2^2	k_2	q_2	h	R_i^2	k_{id}
300	0.9751	0.0258	526.987	0.9902	4.16E−05	376.190	9.43	0.9004	24.34
450	0.9583	0.0244	765.945	0.9951	3.29E−05	566.667	14.62	0.9147	35.66
600	0.9563	0.0240	812.511	0.9961	2.35E−05	789.091	19.46	0.9217	47.26
900	0.9861	0.0202	946.455	0.9986	3.17E−05	909.091	26.18	0.9169	53.06
1200	0.9863	0.0193	966.951	0.9995	3.16E−05	995.269	36.50	0.8938	53.70
1500	0.9547	0.0235	984.011	0.9994	3.99E−05	1111.111	49.26	0.8492	52.35
2000	0.8768	0.0291	1099.005	0.9996	5.56E−05	1227.318	69.44	0.7891	49.06

between the theoretical and experimental capacity (q_2) was observed with $R_2^2 > 0.99$. Also, as seen in Fig. 4, at 100 rpm, all the urea molecules were not fully suspended and hence, increasing the speed to 150 rpm (50%) resulted in significant enhancement in urea uptake. Similarly, the rate constants (k_1, k_2 and k_{id}) for evaluating the effect of initial urea concentration are provided in Table 3. Again, pseudo-second order kinetics best described the sorption system with excellent correlation between the model and the observed q_2 values.

To illustrate the contribution of intra-particle diffusion, BAB urea uptake (q_t) was plotted against $t^{0.5}$ (Fig. 6). The plots indicated that multi-linearity exists within the diffusion system and that three consecutive steps constituted it – step 1 (2.7–5.4 min) involved boundary layer diffusion of urea to the external surface of the BAB; in step 2 (5.4–11.6 min), urea uptake is governed by intra-particle diffusion resistance; and step 3 (12.2–17.3 min) plateaus and allows sorption to equilibrate. Since the diffusion plots did not pass through the origin, it can also be concluded that intra-particle and surface diffusion both control and limit the sorption system.

The mass transfer was evaluated through plots based on Eq. (4) that were found to be linear; the coefficients obtained are presented in Table 4. The significance of urea concentration was once again confirmed by the estimated values of β_L. However, to allow better interpretation of the kinetic data, the procedure detailed by Boyd et al. [31] and Reichenberg [32] was followed, which emphasizes on the three consecutive processes during the adsorption of organics onto porous adsorbents: (i) film diffusion of the sorbate (urea) to the external sorbent surface (BAB), (ii) particle diffusion of urea within the porous BAB surface, and (iii) surface adsorption of urea onto the external surface of the BAB. The last process can be disregarded by assuming it to be very rapid in comparison to the other two; hence, three distinct possibilities emerge:

(i) Film diffusion > particle diffusion
(ii) Film diffusion < particle diffusion
(iii) Film diffusion ≈ particle diffusion

To distinguish this, the mathematical procedure laid out by Reichenberg [32] and Helfferich [33] was used through Eq. (6). F represents the fractional attainment of equilibrium expressed as a ratio of q_t to q_{max}; B, the time constant was evaluated as ($\pi^2 D_i / r_0^2$), where D_i is the effective coefficient of diffusion. The plots of Bt versus t (not shown for brevity) made using Reichenberg's table for concentrations ≤ 1.2 g·L^{-1} did not pass through the origin; this indicated that the rate controlling

Table 4
Mass transfer coefficients and effective diffusivity at various initial concentrations.

C	β_L	D_i
300	3.94E−04	4.3E−10
450	3.63E−04	4.6E−10
600	3.75E−04	4.8E−10
900	4.03E−04	4.9E−10
1200	4.66E−04	5.1E−10
1500	5.22E−04	5.2E−10
2000	6.12E−04	5.2E−10

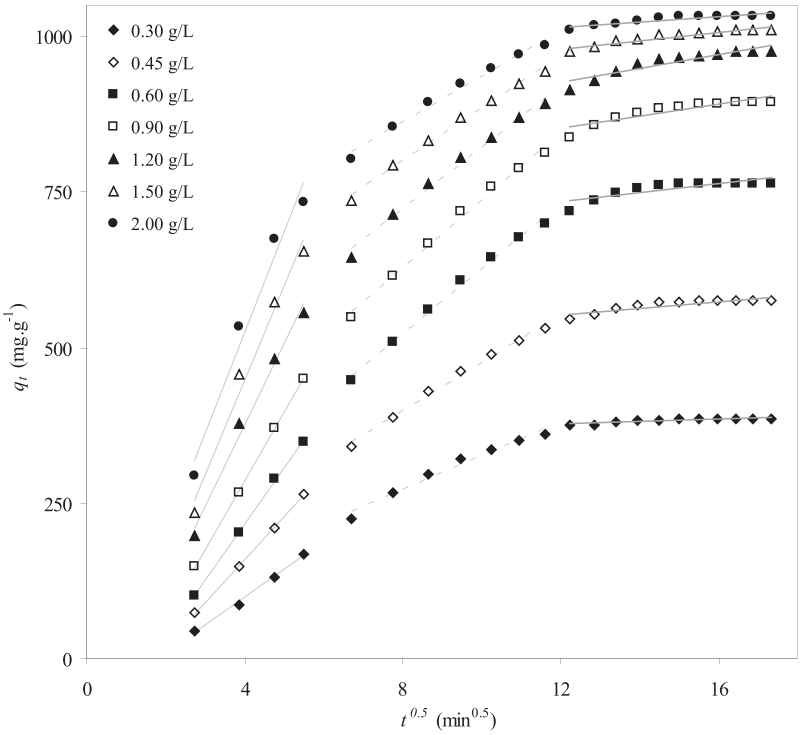

Fig. 6. Intra-particle diffusion plots at various initial urea concentrations.

mechanism was film diffusion. However, at higher urea concentrations, linear plots passed through the origin pointing towards particle diffusion as the governing mechanism. The effective diffusion coefficients evaluated from the slope of the plots, investigated at all the initial concentrations, have been provided in Table 4.

$$F = 1 - \frac{6}{\pi^2}\sum_{n=1}^{\infty}\frac{1}{n^2}exp\left(-n^2 Bt\right) \quad (6)$$

3.4. Isotherm analysis

The experimental data were evaluated against the linearized forms of Langmuir, Freundlich, Flory–Huggins and Dubinin–Radushkevich (DR) isotherm equations and the results are presented in Table 5. As seen, except for the Freundlich model, all the rest provided excellent correlation between predicted and observed urea uptake capacity ($R^2 > 0.95$). However, based on the ND and NSD, it can be seen that the DR model best described the urea sorption onto BAB. Nonetheless, the separation factor (R_L) estimated through the Langmuir model constant was found to lie in the range, $0 < 0.14 < 1$ which was indicative of the sorption's favourability. The Freundlich model which assumes non-ideal and reversible adsorption well-described only the initial and final stages of the sorption; the adsorption intensity (3.08), however, reaffirmed the process spontaneity and favourability. Furthermore, using the Flory–Huggins model constant (K_a), the Gibbs free energy change was calculated as $\Delta G° = RT{\cdot}\ln(K_a)$ and found to be −18 kJ·mol^{-1}. This showed the favourability of urea sorption over its desorption from the BAB surface in addition to affirming its physical nature. The maximum uptake of urea at equilibrium as predicted by the DR model was 1115 mg·g^{-1}, while the Langmuir monolayer capacity was 1150 mg·g^{-1}. Moreover, the mean free energy of sorption calculated using the DR model constant was 3.54 kJ·mol^{-1}, reiterating physisorption as the governing mechanism for urea removal.

Table 5
Isotherm equations and calculated model parameters for urea sorption onto BAB.

Isotherm model	Model parameter	Value
Langmuir isotherm	R^2	0.9753
$\frac{1}{q_e} = \frac{1}{q_m} + \frac{1}{K_L q_m C_e}$	q_m	1150.2
	K_L	0.0051
	R_L	0.1404
	ND	4.7089
	NSD	5.3819
Freundlich isotherm	R^2	0.8727
$log(q_e) = log\,K_F + \left(\frac{1}{n}\right) log\,C_e$	K_F	50.072
	N	3.0851
	ND	10.143
	NSD	11.929
Flory–Huggins	R^2	0.9813
$log\frac{\theta}{C_e} = log(K_a) + m\,log(1-\theta)$	K_a	6.E−04
	ΔG	−18339
	ND	8.0338
	NSD	9.4104
Dubinin–Radushkevich	R^2	0.9988
$ln(q_e) = ln(q_s) - K_{ad}\varepsilon^2$	q_s	1115.8
	k_{ad}	0.0399
	ND	0.9107
	NSD	1.1030

4. Conclusions

The present study elaborated upon the adsorptive potential of Napier grass pyrolysed BAB to immobilize and retain nutrients (urea) from aqueous solutions. It was observed that low temperatures, moderate speed of agitation and high initial urea concentration allowed for greater uptake by the BAB. Kinetic studies on the interaction of the examined parameters with sorption time indicated that the process was exothermic, spontaneous, physical and driven forward through larger concentration difference via pseudo-second-order kinetics. Furthermore, it was concluded that both surface and intra-particle diffusion govern the rate of urea removal from the solution. Also, film diffusion was seen to limit the mass transfer of urea onto the external surface of the BAB. Isotherm analysis of the experimental data pointed towards Dubinin–Radushkevich equation as most appropriate to describe the urea-BAB behaviour with maximum adsorption estimated to be 1115 $mg \cdot g^{-1}$. Hence, this study evaluated the ex-situ potential of Napier grass derived BAB to adsorb, retain and make available, plant-required nutrients from aqueous solutions. It is acknowledged that the conclusions drawn here are specific to both the fertilizer solution investigated (urea) as well as the BAB (Napier grass). Water holding capacity and adsorptive nature of Napier grass BAB signify its importance as soil conditioner. The alkaline nature of Napier grass biochar could show significant effect in terms of growth and biomass generation when applied to acidic soil. It is therefore the recommendation of this study that potential of various other feedstock derived biochar be investigated ex-situ before going for crop field trials. Prior knowledge and quantification could act as an effective screening step and reduce the time as well as effort spent otherwise in long-term field studies.

Acknowledgements

Ashish Yadav and Prithvi Simha acknowledge the University Grants Commission (UGC) and Department of Bioprocess Technology, Institute of Chemical Technology for financial assistance of the project.

References

[1] J. Lehmann, J. Gaunt, M. Rondon, Bio-char sequestration in terrestrial ecosystems – a review, Mitigation Adapt. Strateg. Glob. Change 11 (2006) 395–419.
[2] S. Jeffery, T.M. Bezemer, G. Cornelissen, T.W. Kuyper, J. Lehmann, L. Mommer, et al., The way forward in biochar research: targeting trade-offs between the potential wins, GCB Bioenergy 7 (2015) 1–13.
[3] S.P. Sohi, E. Krull, E. Lopez-Capel, R. Bol, A review of biochar and its use and function in soil, Adv. Agron. 105 (2010) 47–82.
[4] C. Ryu, V.N. Sharifi, J. Swithenbank, Waste pyrolysis and generation of storable char, Int. J. Energy Res. 31 (2007) 177–191.
[5] J.L. Gaunt, J. Lehmann, Energy balance and emissions associated with biochar sequestration and pyrolysis bioenergy production, Environ. Sci. Technol. 42 (2008) 4152–4158.
[6] Intergovernmental Panel on Climate Change (IPCC), in: B. Metz, O.R. Davidson, P.R. Bosch, R. Dave, L.A. Meyer (Eds.), Climate Change 2007: Mitigation: Contribution of Working Group III to the Fourth Assessment Report of the Intergovernmental Panel on Climate Change: Summary for Policymakers and Technical Summary, Cambridge University Press, Cambridge, 2007. <http://www.ipcc.ch/pdf/assessment-report/ar4/wg3/ar4_wg3_full_report.pdf>.
[7] R. Lal, Soil carbon sequestration impacts on global climate change and food security, Science 304 (2004) 1623–1627.
[8] J. Lehmann, A handful of carbon, Nature 447 (2007) 143–144.
[9] M.W. Schmidt, M.S. Torn, S. Abiven, T. Dittmar, G. Guggenberger, I.A. Janssens, et al., Persistence of soil organic matter as an ecosystem property, Nature 478 (2011) 49–56.
[10] B. Glaser, J. Lehmann, W. Zech, Ameliorating physical and chemical properties of highly weathered soils in the tropics with charcoal – a review, Biol. Fertil. Soils 35 (2002) 219–230.
[11] C.J. Atkinson, J.D. Fitzgerald, N.A. Hipps, Potential mechanisms for achieving agricultural benefits from biochar application to temperate soils: a review, Plant Soil 337 (2010) 1–18.
[12] K.Y. Chan, L. Van Zwieten, I. Meszaros, A. Downie, S. Joseph, Agronomic values of greenwaste biochar as a soil amendment, Soil Res. 45 (2008) 629–634.
[13] X.Y. Liu, J.J. Qu, L.Q. Li, A.F. Zhang, Z. Jufeng, J.W. Zheng, et al., Can biochar amendment be an ecological engineering technology to depress N_2O emission in rice paddies? A cross site field experiment from South China, Ecol. Eng. 42 (2012) 168–173.
[14] S. Kumar, R.E. Masto, L.C. Ram, P. Sarkar, J. George, V.A. Selvi, Biochar preparation from Parthenium hysterophorus and its potential use in soil application, Ecol. Eng. 55 (2013) 67–72.
[15] L. Van Zwieten, S. Kimber, S. Morris, K.Y. Chan, A. Downie, J. Rust, et al., Effects of biochar from slow pyrolysis of papermill waste on agronomic performance and soil fertility, Plant Soil 327 (2010) 235–246.
[16] R.L. Tseng, S.K. Tseng, Pore structure and adsorption performance of the KOH-activated carbons prepared from corncob, J. Colloid Interface Sci. 287 (2005) 428–437.
[17] U. Umit, C. Marion, G.H. Ailsa, H.K. Johannes, Physico-chemical characterization of biochars from vacuum pyrolysis of South African agricultural wastes for application as soil amendments, J. Anal. Appl. Pyrolysis 98 (2012) 207–213.
[18] M. Ganesapillai, P. Simha, A. Zabaniotou, Closed-loop fertility cycle: realizing sustainability in sanitation and agricultural production through the design and implementation of nutrient recovery systems for human urine, Sustainable Prod. Consumption 4 (2015) 36–46.
[19] M.G. Pillai, P. Simha, A. Gugalia, Recovering urea from human urine by bio-sorption onto microwave activated carbonized coconut shells: equilibrium, kinetics, optimization and field studies, J. Environ. Chem. Eng. 2 (2014) 46–55.
[20] K. Foo, B.H. Hameed, Insights into the modeling of adsorption isotherm systems, Chem. Eng. J. 156 (2010) 2–10.
[21] M. Ganesapillai, P. Simha, The rationale for alternative fertilization: equilibrium isotherm, kinetics and mass transfer analysis for urea-nitrogen adsorption from cow urine, Resour. Efficient Technol. 1 (2015) 90–97.
[22] G. McKay, S.J. Allen, I.F. McConvey, M.S. Otterburn, Transport processes in the sorption of colored ions by peat particles, J. Colloid Interface Sci. 80 (1981) 323–339.
[23] B. Singh, B.P. Singh, A.L. Cowie, Characterization and evaluation of biochars for their application as a soil amendment, Aust. J. Soil Res. 48 (2010) 516–525.
[24] D.A. Beck, G.R. Johnson, G.A. Spolek, Amending greenroof soil with biochar to affect runoff water quantity and quality, Environ. Pollut. 159 (2011) 2111–2118.
[25] D.A. Laird, P. Fleming, D.D. Davis, R. Horton, B. Wang, D.L. Karlen, Impact of biochar amendments on the quality of a typical Midwestern agricultural soil, Geoderma 158 (2010) 443–449.
[26] A. Dąbrowski, P. Podkościelny, Z. Hubicki, M. Barczak, Adsorption of phenolic compounds by activated carbon – a critical review, Chemosphere 58 (2005) 1049–1070.
[27] Y.C. Chiang, P.C. Chiang, C.P. Huang, Effects of pore structure and temperature on VOC adsorption on activated carbon, Carbon 39 (2001) 523–534.
[28] K. Mohanty, M. Jha, B.C. Meikap, M.N. Biswas, Removal of chromium (VI) from dilute aqueous solutions by activated carbon developed from

Terminalia arjuna nuts activated with zinc chloride, Chem. Eng. Sci. 60 (2005) 3049–3059.

[29] I.A.W. Tan, B.H. Hameed, A.L. Ahmad, Equilibrium and kinetic studies on basic dye adsorption by oil palm fibre activated carbon, Chem. Eng. J. 127 (2007) 111–119.

[30] Y.S. Ho, G. McKay, Sorption of dye from aqueous solution by peat, Chem. Eng. J. 70 (1998) 115–124.

[31] G.E. Boyd, A.W. Adamson, L.S. Meyers, The exchange adsorption of ions from aqueous solution by organic zeolites II; kinetics, J. Am. Chem. Soc. 69 (1947) 2836.

[32] D. Reichenberg, Properties of ion-exchange resins in relation to their structure III; kinetics of exchange, J. Am. Chem. Soc. 75 (1953) 589–592.

[33] H. Helfferich, Ion Exchange, McGraw-Hill, New York, 1962.